One-DOF Origami Boxes with Rigid and Flat Foldability

Chapter · January 2022

DOI: 10.1007/978-3-030-91892-7_8

2 authors:

Yuanqing Gu
Tianjin University
6 PUBLICATIONS **24** CITATIONS
SEE PROFILE

Yan Chen
Tianjin University
44 PUBLICATIONS **486** CITATIONS
SEE PROFILE

One-DOF origami boxes with rigid and flat foldability

Yuanqing Gu [1,2] and Yan Chen [1,2,*]

[1] School of Mechanical Engineering, Tianjin University, Tianjin 300072, China
[2] Key Laboratory of Mechanism Theory and Equipment Design of Ministry of Education, Tianjin University, Tianjin 300072, China
* Corresponding Author. Email: yan_chen@tju.edu.cn, ORCID ID: 0000-0002-4742-6944

Abstract. Rigid origami has great potential in engineering applications to deal with the folding of rigid sheets. Especially in the packaging and transportation industry, origami-inspired box-shaped foldable structures are more advantageous due to the large deployable ratio and low cost. In this paper, a novel crease pattern based on waterbomb pattern is proposed to generate a rigid origami box with flat foldability and a single degree of freedom (DOF). Based on the kinematic equivalence between the rigid origami pattern and the assembly of spherical linkages, kinematic properties of the corresponding integrated mechanism are investigated and formulated. By utilizing the vertex-splitting technique and introducing creases on each vertical facet of an origami box, more box-shaped structures with various geometry and shapes are constructed. In addition, the prototypes of the proposed origami boxes are fabricated to verifying their motion properties. The newly found method can be readily extended to the construction of foldable polygonal prism structures for various engineering applications.

Keywords: Rigid Origami, Crease Pattern, Origami Boxes.

1 Introduction

Origami-inspired foldable structures have been adopted in wide areas including aerospace devices [1], robotics [2], mechanical metamaterials [3], deployable origami tents [4], and so on. Particularly, rigid origami has a better advantage in engineering to deal with the folding of rigid sheets, i.e., its facets revolve around predetermined folds without any deformation during the continuous folding process [5]. From kinematics point of view, the rigid sheets and creases of rigid origami can be regarded as rigid links and revolute joints [6], respectively, e.g. four creases intersect at one point in space can be modeled as a spherical 4*R* (S4*R*) linkage. Therefore, a rigid origami pattern is equivalent to a network of spherical linkages, in which Miura-ori pattern and waterbomb pattern are frequently mentioned and investigated [7]. Apart from rigid foldability, flat foldability of one origami pattern is another important property that needs to be considered to acquire the large deployable ratio and low transportation cost [8], which refers to the capability to fold an origami pattern compactly into a flat overlapped sheet.

Folding rigid origami boxes or cartons is challenging and practical in both theoretical investigation and engineering application. Yet, there is little work on how to fold boxes

and cartons rigidly and compactly into a flat overlapped configuration. Balkcom et al. [9] presented two rigid folding schemes for cubical bags but with specific height conditions. The first practical solution for rigid tall shopping bags was proposed by Wu and You [10], which can lead to direct applications in the packaging industry. On the other hand, kinematics analysis and stiffness characteristics have been demonstrated for folding the patterned sheets into box-shaped cartons of complex geometry and shapes [11,12]. Furthermore, origami-inspired mechanisms related to three-dimensional crease patterns have been developed to provide more design inspiration [13,14].

The crease patterns that enable origami cubes rigid and flat foldability with mobility one have been proposed in our previous work [15]. In order to enhance the engineering applications of origami structures such as foldable boxes, cartons and containers, this paper for the first time presents an approach to construct the novel crease patterns for origami box-shaped structures with various geometry.

The layout of the paper is as follows. Section 2 proposes a novel origami box based on waterbomb pattern. The variants of origami boxes are presented in Section 3, and the conclusion and further discussion are given in Section 4.

2 An origami box with the novel crease pattern

The well-known crease pattern of a waterbomb origami in Fig. 1(a) is obtained by tessellating six-crease origami vertices, where the dashed lines stand for mountain creases and the solid lines denote valley creases. Here, we take a part of simplified crease pattern, highlighted in red line area in Fig. 1(a), as the planer net of a box with a square base (Fig. 1(b)), a crease pattern of the novel origami box is constructed in Fig. 1(c).

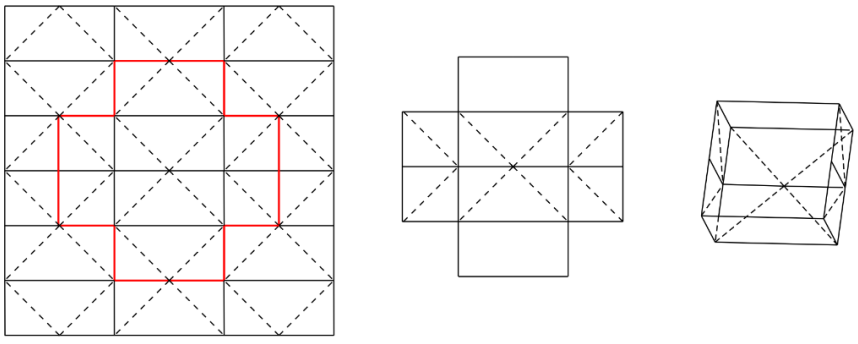

Fig. 1. (a) Crease pattern of a waterbomb origami. (b) The planer net of (c) a novel origami box with a square base.

On the base of this origami box, see Fig. 2, vertices A, B, C and D with identical geometry can be modelled as one-DOF S4*R* linkages, respectively. The identical six-crease vertices E and F can be modelled as S6*R* linkages, so do vertex G. Although vertices E, F, and G are all derived from waterbomb pattern, the initial configuration of vertices E and F are not flat in the fully deployable state of the box.

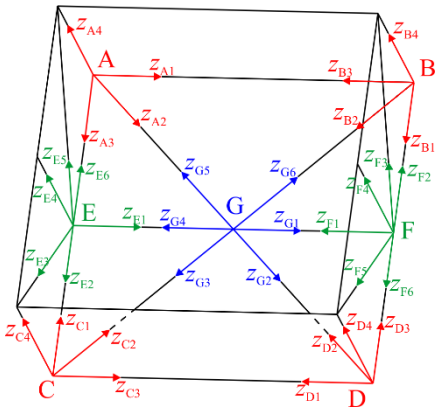

Fig. 2. The 4*R*-4*R*-4*R*-4*R*-6*R*-6*R*-6*R* integrated mechanism.

Nonetheless, the 4*R*-4*R*-4*R*-4*R*-6*R*-6*R*-6*R* (from vertices A to G) integrated mechanism is formed on the bottom of this origami box as shown in Fig. 2. Kinematic analysis of this integrated mechanism is carried out based on the matrix method with the D-H notations [16]. With this method, Fig. 3(a) shows the D-H parameters of a portion of a general spherical linkage, whose rotating axes intersect at one point in space. For a single closed loop linkage, the closure equation can be found in [16] as

$$\mathbf{Q}_{21}\mathbf{Q}_{32}\mathbf{Q}_{43}...\mathbf{Q}_{i(i-1)}\mathbf{Q}_{1i}=\mathbf{I}. \tag{1}$$

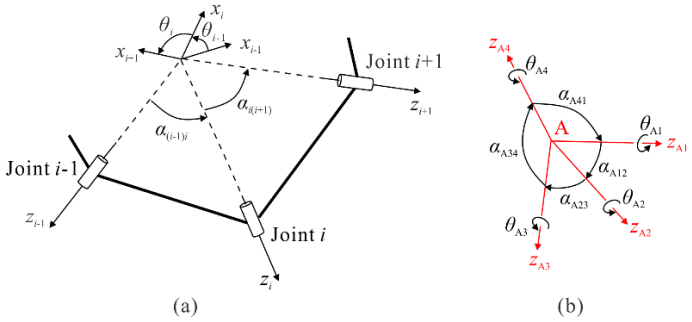

Fig. 3. The D-H notations of (a) a portion of a spherical linkage and (b) the S4*R* linkage A.

Take the S4*R* linkage A in Fig. 3(b) as an example, the geometrical parameters of the S4*R* linkages are identified as

$$\alpha_{i12}=\alpha_{i23}=\pi/4\,,\ \alpha_{i34}=\alpha_{i41}=\pi/2\,, \tag{2}$$

in which i = A, B, C, D.

For S6*R* linkages E and F, there exists

$$\alpha_{i12}=\alpha_{i61}=\pi/2\,,\ \alpha_{i23}=\alpha_{i34}=\alpha_{i45}=\alpha_{i56}=\pi/4\ (i=\mathrm{E,\ F})\,, \tag{3}$$

and for S6*R* linkage G,

$$\alpha_{\mathrm{G23}}=\alpha_{\mathrm{G56}}=\pi/2\,,\ \alpha_{\mathrm{G12}}=\alpha_{\mathrm{G34}}=\alpha_{\mathrm{G45}}=\alpha_{\mathrm{G61}}=\pi/4\,. \tag{4}$$

Kinematics of each spherical linkage can be deduced through the above closure equation and geometric parameters. Firstly, the joint angle relationships of the S4*R* linkages can be derived as

$$\tan\frac{\theta_{i2}}{2}=\left(\sqrt{2}\tan\theta_{i1}\right)^{-1},\ \theta_{i3}=\theta_{i1},\ \ \tan\frac{\theta_{i4}}{2}=\left(\sin\theta_{i1}\right)^{-1}\ (i=\text{A, B, C, D}). \tag{5}$$

As linkages A and B share a common revolute joint, so do linkages C and D, there exit further relations that

$$\theta_{\text{A1}}=\theta_{\text{B3}},\ \theta_{\text{C3}}=\theta_{\text{D1}} \tag{6a}$$

$$\theta_{\text{A}j}=\theta_{\text{B}j},\ \theta_{\text{C}j}=\theta_{\text{D}j}\ \ (j=1, 2, 3, 4). \tag{6b}$$

Subsequently, $\theta_{\text{A2}},\theta_{\text{B2}},\theta_{\text{C2}}$ and θ_{D2} can be obtained as inputs of linkage G, so we can obtain the following relationships as

$$\theta_{\text{G2}}=\theta_{\text{D2}},\ \theta_{\text{G3}}=\theta_{\text{C2}},\ \theta_{\text{G5}}=\theta_{\text{A2}},\ \theta_{\text{G6}}=\theta_{\text{B2}}, \tag{7a}$$

$$\tan\frac{\theta_{\text{G1}}}{2}=\tan\frac{\theta_{\text{G4}}}{2}=-\frac{\sqrt{2}}{2}\tan\frac{\theta_{\text{G2}}}{2},\ \theta_{\text{G2}}=\theta_{\text{G3}}=\theta_{\text{G5}}=\theta_{\text{G6}}, \tag{7b}$$

which further leads to

$$\theta_{\text{A}j}=\theta_{\text{B}j}=\theta_{\text{C}j}=\theta_{\text{D}j}\ \ (j=1, 2, 3, 4). \tag{8}$$

Similarly, due to the relations at common revolute joints of linkages E and F,

$$\theta_{\text{E1}}=\theta_{\text{G4}},\ \theta_{\text{E2}}=\theta_{\text{C1}},\ \theta_{\text{E6}}=\theta_{\text{A3}}, \tag{9a}$$

$$\theta_{\text{F1}}=\theta_{\text{G1}},\ \theta_{\text{F2}}=\theta_{\text{B1}},\ \theta_{\text{F6}}=\theta_{\text{D3}}, \tag{9b}$$

we can also derive that

$$\cos\theta_{\text{E4}}=(\cos\theta_{\text{E1}}-1)\cos^2\theta_{\text{E2}}-2\sin\theta_{\text{E1}}\sin\theta_{\text{E2}}+1, \tag{10a}$$

$$\tan\frac{\theta_{\text{E3}}}{2}=\tan\frac{\theta_{\text{E5}}}{2}=\frac{-\sqrt{2}\sin\theta_{\text{E4}}+\sqrt{\begin{array}{l}2\sin^2\theta_{\text{E4}}+\left(\cos\theta_{\text{E4}}+1\right)^2\\-\left(2\cos\theta_{\text{E1}}+1-2\sin\theta_{\text{E1}}\sin\theta_{\text{E2}}-\cos\theta_{\text{E4}}\right)^2\end{array}}}{2\left(\cos\theta_{\text{E1}}+1-\sin\theta_{\text{E1}}\sin\theta_{\text{E2}}\right)}, \tag{10b}$$

and the following relations can be given by combining equations (7-10) as

$$\theta_{\text{E}j}=\theta_{\text{F}j}\ \ (j=1, 2, ..., 6). \tag{11}$$

From the above analysis, it can be seen that θ_{A1} is the only input of this integrated mechanism and the rest of joint angles can be determined by θ_{A1}. Hence, the proposed origami box has mobility one. Furthermore, dihedral angles are preferred to directly represent the folding motion, which can be expressed with respect to the joint angles as

$$\varphi_{i1}=\pi+\theta_{i1},\ \varphi_{i2}=\pi-\theta_{i2},\ \varphi_{i3}=\pi+\theta_{i3},\ \varphi_{i4}=\pi+\theta_{i4}\ \ i=\text{A, B, C, D}. \tag{12a}$$

$$\varphi_{\text{G1}}=\pi+\theta_{\text{G1}},\ \varphi_{\text{G2}}=\pi-\theta_{\text{G2}},\ \varphi_{\text{G3}}=\pi-\theta_{\text{G3}},\ \varphi_{\text{G4}}=\pi+\theta_{\text{G4}},\ \varphi_{\text{G5}}=\pi-\theta_{\text{G5}},\ \varphi_{\text{G6}}=\pi-\theta_{\text{G6}}, \tag{12b}$$

$$\varphi_{\text{E1}}=\pi+\theta_{\text{E1}},\ \varphi_{\text{E2}}=\pi+\theta_{\text{E2}},\ \varphi_{\text{E3}}=\pi-\theta_{\text{E3}},\ \varphi_{\text{E4}}=\pi+\theta_{\text{E4}},\ \varphi_{\text{E5}}=\pi-\theta_{\text{E5}},\ \varphi_{\text{E6}}=\pi+\theta_{\text{E6}}, \tag{12c}$$

$$\varphi_{\text{F1}}=\pi+\theta_{\text{F1}},\ \varphi_{\text{F2}}=\pi+\theta_{\text{F2}},\ \varphi_{\text{F3}}=\pi-\theta_{\text{F3}},\ \varphi_{\text{F4}}=\pi+\theta_{\text{F4}},\ \varphi_{\text{F5}}=\pi-\theta_{\text{F5}},\ \varphi_{\text{F6}}=\pi+\theta_{\text{F6}}. \tag{12d}$$

Hence, the kinematic relations of dihedral angles in this one-DOF origami box are presented as following equations. Given φ_{A1} as an input dihedral angle, the input-output curves of dihedral angles in this origami box are obtained and illustrated in Fig. 4. A physical prototype with flat foldability has been fabricated to demonstrate and verify the symmetric motion as shown in Fig. 5.

$$\tan\frac{\varphi_{i2}}{2}=\sqrt{2}\tan\varphi_{i1},\ \theta_{i3}=\theta_{i1},\ \ \tan\frac{\varphi_{i4}}{2}=\sin\varphi_{i1}\ (i=\mathrm{A,\ B,\ C,\ D}),$$

$$\varphi_{\mathrm{A}j}=\varphi_{\mathrm{B}j}=\varphi_{\mathrm{C}j}=\varphi_{\mathrm{D}j}\ \ (j=1,\ 2,\ 3,\ 4),$$

$$\varphi_{\mathrm{G}2}=\varphi_{\mathrm{G}3}=\varphi_{\mathrm{G}5}=\varphi_{\mathrm{G}6}=\varphi_{\mathrm{A}2},\ \tan\frac{\varphi_{\mathrm{G}1}}{2}=\tan\frac{\varphi_{\mathrm{G}4}}{2}=\sqrt{2}\tan\frac{\varphi_{\mathrm{G}2}}{2},$$

$$\varphi_{\mathrm{E}1}=\varphi_{\mathrm{G}4},\ \varphi_{\mathrm{E}2}=\varphi_{\mathrm{E}6}=\varphi_{\mathrm{A}3},$$

$$\cos\varphi_{\mathrm{E}4}=(\cos\varphi_{\mathrm{E}1}+1)\cos^2\varphi_{\mathrm{E}2}+2\sin\varphi_{\mathrm{E}1}\sin\varphi_{\mathrm{E}2}-1,$$

$$\tan\frac{\varphi_{\mathrm{E}3}}{2}=\tan\frac{\varphi_{\mathrm{E}5}}{2}=\frac{2\left(1-\cos\varphi_{\mathrm{E}1}-\sin\varphi_{\mathrm{E}1}\sin\varphi_{\mathrm{E}2}\right)}{\sqrt{2}\sin\varphi_{\mathrm{E}4}+\sqrt{2\sin^2\varphi_{\mathrm{E}4}+\left(1-\cos\varphi_{\mathrm{E}4}\right)^2-\left(1-2\cos\varphi_{\mathrm{E}1}-2\sin\varphi_{\mathrm{E}1}\sin\varphi_{\mathrm{E}2}+\cos\varphi_{\mathrm{E}4}\right)^2}},$$

$$\varphi_{\mathrm{E}j}=\varphi_{\mathrm{F}j}\ \ (j=1,\ 2,\ ...,6).\qquad(13)$$

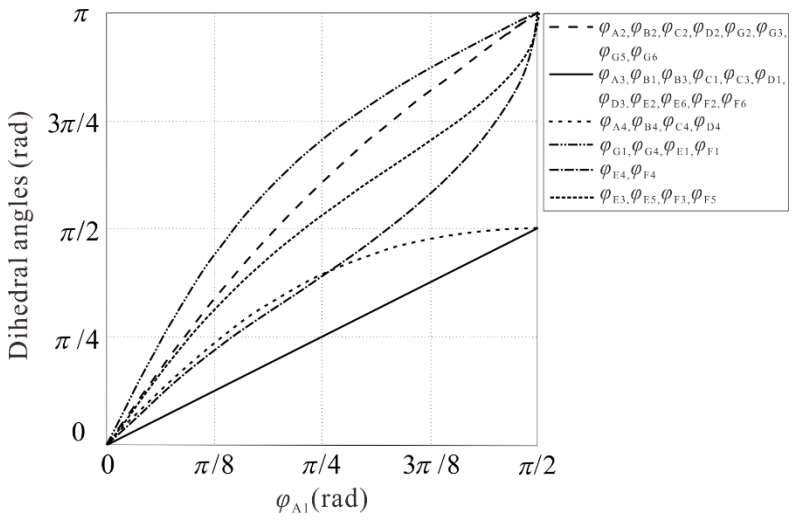

Fig. 4. Input-output curves of dihedral angles in the proposed origami box.

Fig. 5. Phototype of the origami box and its folding process.

3 The variants of origami boxes

For the proposed crease pattern of origami box with a square base in Fig. 2, vertex-splitting technique [17] is adopted to construct the one-DOF and flat foldable origami boxes with distinct geometry. As shown in Fig. 6, by splitting six-crease vertex G, two four-crease vertices G_1 and G_2 connected by a common crease line (revolute joint) are obtained to form the rectangle base of the cuboid box. Kinematic equivalence and symmetric folding of the assembly of those two four-crease vertices have been revealed in [17], so one-DOF rigid and flat foldability is preserved in this cuboid box. In addition, by adjusting the geometric parameters of six-crease vertices E and F, the extended origami box with a symmetric hexagon base (as an example) has been identified and constructed in Fig. 7, which demonstrates the flexibility of our design approach in this paper. Noted that the purpose of vertex-splitting technique used in origami boxes is to extend the geometry of the flat foldable boxes for wider applications.

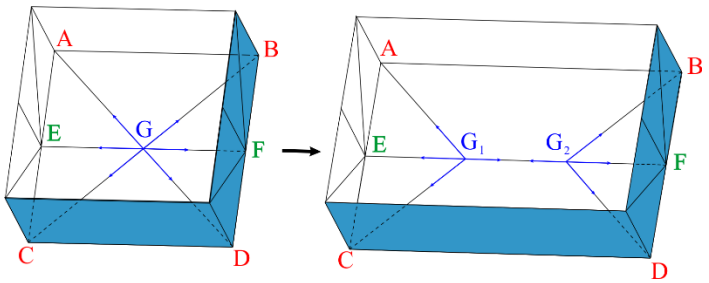

Fig. 6. The origami cuboid box with vertex-splitting technique.

Fig.7. The extended origami box with a symmetric hexagon base.

Further, inspired by the proposed design method for origami cube in our previous work [15], we aim to construct various polygonal prism structures by introducing creases on each vertical facet of an origami box respectively. The crease patterns of pentagonal and hexagonal origami prism structures are shown in Fig. 8, in which the geometry conditions of flat foldability at each origami vertex should always be considered. The same approach described in Section 2 can also be utilized to analyse the kinematics in those origami prism structures.

For example, compared with the box in Fig. 2, four-crease vertices A and C have identical geometry in this hexagonal origami prism structure, so do vertices B and D. Here, four-crease vertex G becomes one S4*R* linkage, where each one is one-DOF. As sharing common creases, AB, BG, GD and DC, the motion of the assembly of those five S4*R* linkages can be obtained and identified if only one kinematic input is given to it. Meanwhile, the motion of three-DOF S6*R* linkage at vertex E is determined by the three inputs from vertices A, G and C, respectively. For vertex F, the motion is also defined from vertices B, G and D. Hence, the hexagonal origami prism structure has mobility one. The folding process of the physical model is shown in Fig. 9, which presents the plane-symmetric folding performance of this origami prism structure due to the symmetric layout of all the creases.

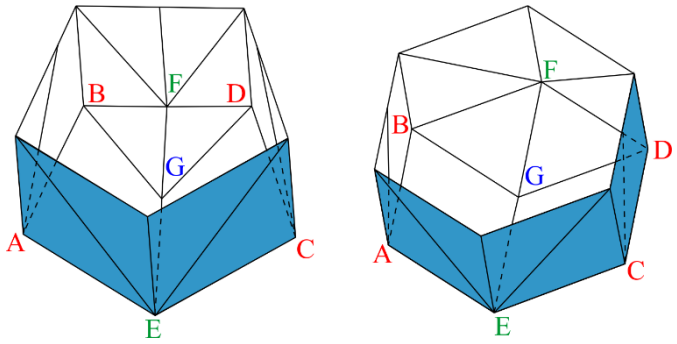

Fig. 8. The crease patterns of pentagonal and hexagonal origami prism structures.

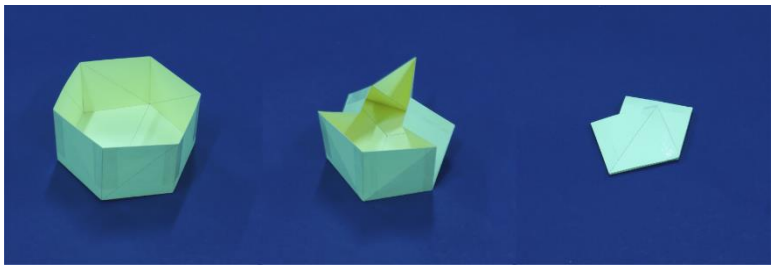

Fig. 9. Folding process of hexagonal origami prism structures.

4 Conclusions and discussion

In this paper, a novel origami box with one-DOF rigid and flat foldability has been proposed based on waterbomb pattern. Kinematics of the corresponding integrated mechanism has been investigated based on the kinematic equivalence between rigid origami pattern and the assembly of spherical linkages. Furthermore, more origami box-shaped structures with various geometry and shapes are developed by utilizing vertex-splitting technique and introducing additional creases. Physical models have been fabricated to reveal the folding process and validate the proposed approach.

Due to the folding motion derives from the motion of the integrated mechanism at the bottom of each origami box, the height of foldable structures can be selected without physical interference. In addition to folding the origami boxes, the new method proposed in this paper can be readily extended to construct deployable polyhedral structures for wider engineering applications including temporary aerospace residences, small satellites, containers, etc.

References

1. Morgan, J., Magleby, S.P., Howell, L.L.: An approach to designing origami-adapted aerospace mechanisms. J. Mech. Des. 138 (5), p. 052301 (2016).
2. Felton, S., Tolley, M., Demaine, E., Rus, D., Wood, R.: A method for building self-folding machines. Science 345 (6197), 644-646 (2014).
3. Fang, H., Chu, S.C.A., Xia, Y., Wang, K.W.: Programmable self-locking origami mechanical metamaterials. Adv. Mater. 30,1706311 (2018).
4. Liu, S., Lv, W., Chen, Y., Lu, G.: Deployable prismatic structures with rigid origami patterns. J. Mech. Robotics 8, 031002 (2016).
5. Wang, K., Chen, Y.: Folding a patterned cylinder by rigid origami. In: Wang-Iverson, P., Lang, R., Yim, M. (eds.) Origami 5, AK Peters/CRC Press, pp. 265–276. New York (2011).
6. Dai, J.S., Rees Jones, J.: Mobility in metamorphic mechanisms of foldable/erectable kinds. J. Mech. Des. 121, 375–382 (1999).
7. Feng, H., Ma, J., Yan, C., You, Z.: Twist of tubular mechanical metamaterials based on waterbomb origami. Scientific Reports 8(1), 9522 (2018).
8. Tachi, T.: Freeform variations of origami. J. Geom. Graph. 14, 203–215 (2010).
9. Balkcom, D.J., Demaine, E.D., Demaine, M.L., Ochsendorf, J.A., You, Z.: Folding paper shopping bags. In: Origami4. Proceedings of the 4th International Meeting of Origami Science, Math, and Education, pp. 315–334 (2009).
10. Wu, W., You, Z.: A solution for folding rigid tall shopping bags. Proc. R. Soc. A 467, 2561–2574 (2011).
11. Dai, J. S., Rees Jones, J.: Kinematics and mobility analysis of carton folds in packing manipulation. Proc. Inst. Mech. Eng., Part C: J. Mech. Eng. Sci. 216(C10), 959–970 (2003).
12. Dai, J. S., Cannella, F.: Stiffness characteristics of carton folds for packaging. J. Mech. Des. Trans. 130, 022305 (2008)
13. Wei, G., Dai, J.S.: Origami-inspired integrated planar-spherical overconstrained mechanisms, J. Mech. Des. 136 (5), 051003(2014).
14. Chen, Y., Lv, W., Peng, R., Wei, G.: Mobile assemblies of four-spherical-4R-integrated linkages and the associated four-crease-integrated rigid origami patterns. Mech. Mach. Theory 142, 103613 (2019).
15. Gu, Y., Chen, Y.: Origami cubes with one-DOF rigid and flat foldability. Int. J. Solids Struct. 207, 250-261 (2020).
16. Denavit, J., Hartenberg, R.S.: A kinematic notation for lower-pair mechanisms based on matrices. Trans. ASME J. Appl. Mech. 22, 215–221(1955).
17. Zhang, X., Chen, Y.: Vertex-splitting on a diamond origami pattern. J. Mech. Rob. 11(3), 031014 (2019).